

## Influence of Nanodispersed Organoclay on Rheological and Swelling Properties of Ethylene Propylene Diene Terpolymer

Himadri Acharya and Suneel K. Srivastava\*

Department of Chemistry, Indian Institute of Technology, Kharagpur - 721302, India

Received June 15, 2005; Revised October 31, 2005

**Abstract:** The dispersion of organoclay in ethylene propylene diene terpolymer (EPDM) matrix was correlated with the rheological and swelling properties of nanocomposites. X-ray diffraction pattern (XRD) and transmission electron microscopic (TEM) analysis exhibited the disordered-intercalated structure of EPDM/organoclay nanocomposite. The extent of the disordered phase increased with increasing organoclay content up to a limiting value of 3 wt% after which equilibrium tended towards intercalation. The dispersion effect of organoclay in EPDM matrix was clarified by the physicochemical properties like rheological response and swelling thermodynamics in toluene. The increase in viscoelastic properties of EPDM nanocomposite with increasing organoclay content up to 3 wt%, followed by a subsequent decrease up to 4 wt%, was correlated in terms of the disordered and ordered states of the dispersed nano-clay sheets. Swelling measurements revealed that the change in entropy of the swelling increased with the increase in disorder level but decreased with the increase in intercalation level of organoclay in the disordered-intercalated nanocomposite. The increase in solvent uptake was comparable with the free volume in EPDM matrix upon inclusion of silicate particles, whereas the inhibition in solvent uptake for higher organoclay loading was described by bridging flocculation.

*Keywords:* nanocomposites, organoclay, dispersion, rheology, swelling behavior.

### Introduction

Nanocomposite in general is a combination of more than one phase of different materials of which one is in nanometric level. Toyota research group first synthesized nylon-6 nanocomposite having small amount of exfoliated organoclay throughout the nylon-6 polymer matrix.<sup>1</sup> These modified materials are very different from conventional composites in the light of their microstructure and properties enhancement. In this regards, composite with nanoscale inorganic particle distribution in polymer matrix have attracted considerable technological and scientific interest through the effective way of molecular interaction between the matrix and filler to manipulate an organic-inorganic nanosystem.<sup>2-4</sup> In most of the polymer nanocomposites, clay minerals have extensively been used as the reinforcing agent due to its cheapness and easy availability. In addition, nanoscale sizes of the clay components create a high surface-to-volume ratio<sup>5</sup> providing thereby strong interaction between the polymer and silicate layers. This result in a greater miscibility of the different phases and leads to the high performing materials with the improvement in physico-chemical properties like mechani-

cal, thermal, barrier and flame retardant properties of the polymer.<sup>6-10</sup> Structure and properties of these nanocomposites are guided by the compatibility of polymer matrix with layered silicates having  $\approx 1$  nm thickness of silicate platelets. Sodium montmorillonite, an inorganic layered materials belongs to the (2:1) phyllosilicate family where positively charged sodium ions are sandwiched between the negatively silicate layers. Organic cations (organo ammonium or organo phosphonium) are intercalated in the interlayer by exertion of  $\text{Na}^+$  ions to make the inorganic materials more compatible with the organic polymer matrix. The insertion of long chain alkylammonium ion enlarges the spacing between the silicate sheets and also brings the hydrophilic clay to hydrophobic in nature. This organic cation exchanged silicate layers are easily dispersed in the non-aqueous medium. The neighboring silicate sheets are connected by polymer chains to form either intercalated nanocomposite where the regular insertion of polymer chains in the interlayer or exfoliated nanocomposite where silicate layers are distributed randomly throughout the polymer matrix. In addition, the quasi-regular distribution of silicate layers results the formation of partially intercalated nanocomposites where both the exfoliated and intercalated configuration co-exists.<sup>11-13</sup> Degree and type of dispersion of clay particles determine the nanocomposites properties.<sup>14,15</sup> In

\*Corresponding Author. E-mail: sunit@chem.iitkgp.ernet.in

our earlier work, we reported the thermally and mechanically reinforced EPDM/organoclay nanocomposites containing 16Me-MMT.<sup>16</sup> From the processing and application point of view it is further desirable to correlate the physico-chemical properties with the microstructure of the nanocomposites. The rheological response of nanocomposites is related to the distortion or deformation of the matrix.<sup>17</sup> The present work, therefore, aims at investigating the dispersion effect of different silicate loading to the rheological properties in disordered-intercalated EPDM/organoclay nanocomposites and the surface interaction between the polymer chain and organoclay. Further, the influence of silicate layers of nano-meter scale towards the swelling ability of EPDM in toluene at room temperature have also been investigated in terms of volume uptake and cross-linking density along with two important thermodynamic parameters, i.e., free energy change ( $\Delta G_{sw}$ ) and the change in entropy ( $\Delta S_{sw}$ ). The driving force for the swelling is the increase in entropy, which occurs as polymer network chains spread apart and swell with the penetrated solvent molecules.

## Experimental

**Preparation of Nanocomposites.** The materials and preparation procedure of EPDM/organoclay nanocomposite materials were described in our previous publication.<sup>16</sup> The nanocomposites were prepared by first converting the silicate surface of sodium montmorillonite from a hydrophilic to organophilic by ion exchange of inorganic cations with hexadecyl ammonium ion. Thus prepared organophilic clay (16Me-MMT) dispersion in toluene was added to the solution of EPDM in toluene with vigorous stirring at 90 °C. After 2 h, 1.0 wt% of 40% dicumyl peroxide (DiCup 40C) was added to it and the mixture was dried and finally compressed at 150 °C for 45 min. Plaques with various EPDM composites containing 0, 2, 4, 6 and 8 wt% of 16Me-MMT have been prepared and designated as EM0, EM2, EM3, EM4 and EM8 respectively.

**X-ray Diffraction (XRD).** X-ray diffraction studies were performed by using a Rigaku Miniflex diffractometer (30 kV, 10 mA) with Cu K $\alpha$  radiation in the  $2\theta$  ranges 2–8° at a scanning range of 2°/min at room temperature.

**Transmission Electron Microscopy (TEM).** The dispersion of organophilic clay in the EPDM matrix and the nanostructure were observed through microscopic investigations on a JEOL (JEM 3010) transmission electron microscope (TEM).

**Rheological Characterization.** The rheological measurements of the nanocomposites were performed using an ARES parallel plate Rheometer, Rheometric Scientific, Piscataway, NJ, USA. Dynamic frequency sweep isothermal measurements were performed in the frequency range 1–250 rad/s using strain amplitude of 1% at 25 °C. In the master curves, the storage modulus,  $G'$  refers to reversibly stored strain

energy in the nanocomposites and the loss modulus,  $G''$  stands for the amount of energy given off by the nanocomposites irreversibly to its environment.

**Swelling Characterization.** Technique used for the swelling measurement is based on gravimetric method as discussed in ASTM D2765-95 (Method C). Carefully weighed ( $w_i$ ) samples were immersed in toluene at 25 °C. After equilibrium swelling the samples were taken out and again carefully weighed ( $w_s$ ) and the solvent uptake ( $Q_e$ ) was computed using the equation

$$Q_e = \frac{(w_s - w_i)/w_i}{M_s} \times 100 \quad (1)$$

where,  $M_s$  was the molar mass of the solvent.

## Results and Discussion

**XRD and TEM Analysis.** XRD pattern of the 16Me-MMT and EPDM composites are displayed in Figure 1. It is

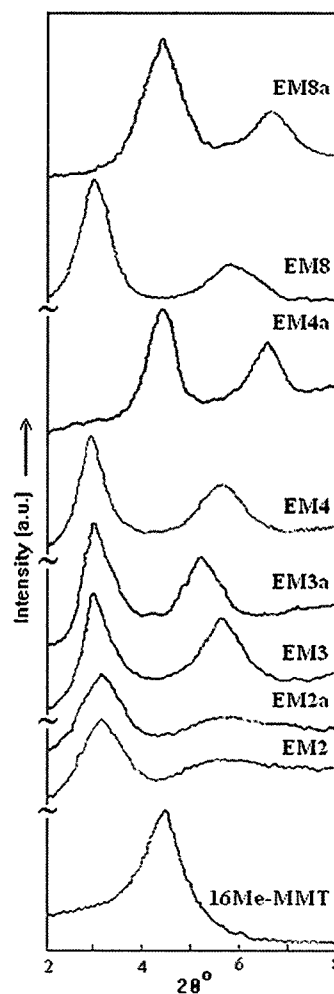


**Figure 1.** XRD patterns of 16Me-MMT and EPDM nanocomposites before and after swelling in toluene.

clearly observed that all the composites shows the 001 reflection peak at  $2\theta \approx 3.0^\circ$  ( $d_{001} = 2.95$  nm). Shifts in basal reflection peak from  $2\theta = 4.5^\circ$  to  $3.0^\circ$  of organophilic clay in EPDM composites confirm the intercalation of EPDM chain between the silicate layers. It also shows that basal reflection peak of composite containing 2 wt% of organoclay is less intense. This is probably due to its dependence on many parameters such as content of clay, orientation of the clay, and exfoliation extent, i.e. dispersion of silicate layers in EPDM matrix. The nanocomposites above 2 wt% still exhibits registry associated with original crystallites. In the present case, such a layer correlation is not detectable by XRD and, therefore, correct characterization requires microscopy. The presence of another peak at around  $2\theta = 5.5^\circ$  indicates the compression of silicate gallery height. Such a decrease in  $d$  spacing of silicate layers of MMT dispersed in EPDM matrix could be attributed to the partial decomposition of the hexadecyl ammonium ion and expulsion of the ammonium salt during preparation under thermal condition leading to the collapse of the organoclay interlayer distance.<sup>18</sup>

EM2a, EM3a, EM4a and EM8a are the X-ray diffractogram of the corresponding nanocomposites after equilibrium swelling in toluene. From the figure it is clear that when the solvent penetrate through the silicate gallery of nanocomposite containing more than 3 wt% organoclay, the domain spacing collapses, though, the amount of EPDM chains inside the clay layers and the degree of exfoliation inside the clay layer are likely to be same regardless of the total amount of the clays. Such behaviour could account from the change in relative proportion of disordered and intercalated species with the filler content. According to the recently reported work,<sup>2,33,37</sup> distribution of platelets has an intrinsic tendency towards becoming ordered from disordered state spontaneously with the filler contents with a crossover at which equal amounts of the disordered and ordered phases are expected. Therefore, it appears that the formation of more favorable intercalated phase in EPDM nanocomposites containing 16Me-MMT more than 3 wt% plays an important role for the collapse of the domain spacing. This may be attributed to the bridging flocculation where the polymer chain stretches out and extraction of the unvulcanized rubber intercalated between the silicate layers during swelling. However, more investigations are needed to explain this interesting behaviour quantitatively. Table I also records the

**Table I. Gel Fraction Data for the EPDM Nanocomposites with Various wt% of 16Me-MMT Loading**

Sample	Gel Fraction (%)
EM0	97.84
EM2	92.64
EM3	88.63
EM4	87.70
EM8	85.36

gel fraction data of the unfilled rubber as well as its nanocomposites with different clay loading.

However X-ray diffractogram provides a partial picture about the distribution of organomodified nanoclay in disordered-intercalated polymer nanocomposite. However, the XRD can only detect the parallel ordered stacking of silicate layers. Therefore, a complete characterization of nanocomposite morphology requires microscopic investigation. Figure 2 shows the TEM images of EPDM/organoclay composite containing 3 and 8 wt% of organoclay, which depicts the presence of disordered and intercalated clay tactoids.

**Rheological Properties.** In a linear viscoelastic regime with a preset strain ( $\gamma_0$ ), the time dependent stress  $\tau(t)$  arises due to deformation is represented by<sup>19-21</sup>

$$\tau(t) = \gamma_0 \{ G'(\omega) \sin(\omega t) + G''(\omega) \cos(\omega t) \} \quad (2)$$

where,  $\omega$  is the frequency and  $t$  is the real time. The  $\tan\delta = G''/G'$ , is the ratio between the viscous and elastic response of the materials.  $\tan\delta$  is very large ( $\gg 1$ ) for liquid-like materials and very small ( $\ll 1$ ) for solid-like materials.<sup>22</sup> The viscosity function is the ratio of the strain to the stress rate. The overall magnitude of the complex viscosity is given by

$$|\eta^*| = \langle (\eta')^2 + (\eta'')^2 \rangle^{1/2} \quad (3)$$

$\eta^*$  is the complex viscosity,  $\eta' = G''/\omega$  is the viscous portion of complex viscosity and  $\eta'' = G'/\omega$  is the elastic portion of the complex viscosity.

Figure 3(a) shows the variation of  $(\eta^*)$  versus frequency ( $\omega$ ) of EPDM nanocomposites at different clay percent. It is seen that the complex viscosity is relatively low for pure EPDM than its organoclay nanocomposites and it increases monotonically with increase in clay concentration up to 3 wt% in EPDM matrix; beyond which further clay loading results the decrease in viscosity. This suggests the higher clay dispersion and disordered level dominates up to 3 wt% with stronger EPDM-layered silicate interactions and greater ori-

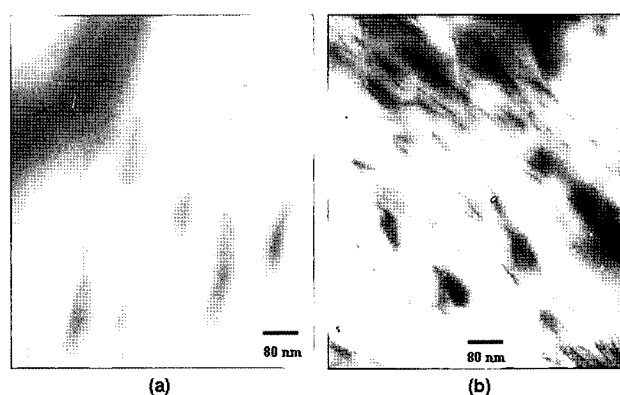


**Figure 2.** TEM images of EPDM nanocomposites containing (a) 3 wt% 16Me-MMT and (b) 8 wt% 16Me-MMT.

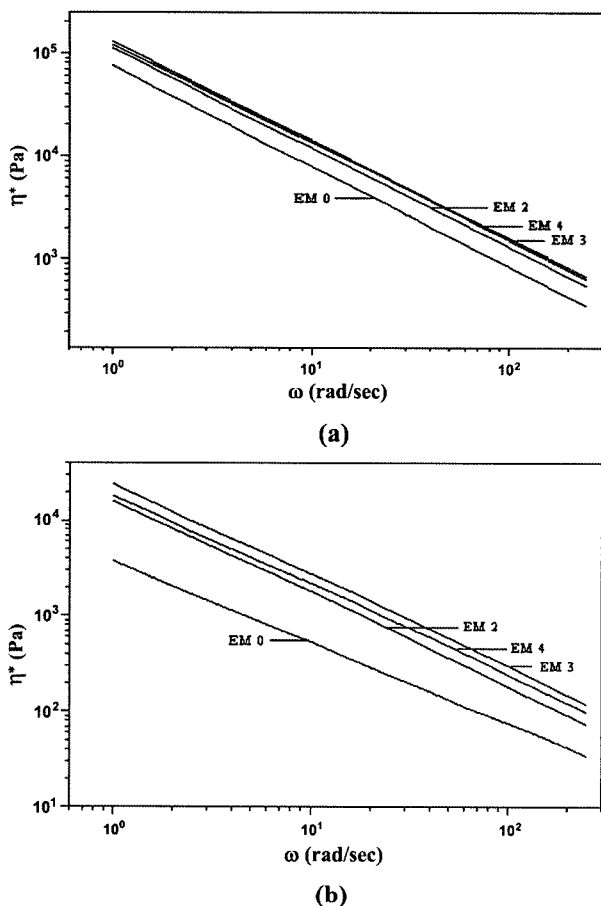


**Figure 3.** (a) Complex viscosity and (b) dynamic viscosity for EPDM nanocomposites containing various wt% of 16Me-MMT content.

entation in the disordered-intercalated nanocomposites. Above the 3 wt% of organoclay loading, the silicate platelets aligned in more ordered state and oriented in similar fashion suppress the viscosity.<sup>23-25</sup> According to Onsager,<sup>26</sup> increase in organoclay content in polymer matrix the silicate platelets possess inherent trend to become ordered from disordered state. Dimerzio *et al.*<sup>27</sup> also predicted the crossover organoclay content at which equal amount of ordered and disordered phases are expected for polyisoprene/organoclay nanocomposites is 3.2. Accordingly, the disordered phases are more favorable and predominate in determining the properties of nanocomposites below this crossover clay content as already observed in our case.

Figure 3(b) shows the dynamic viscosity ( $\eta'$ ) of the nanocomposites for a range of organoclay content. It is observed from the figure that the nanocomposites shows more shear thinning behaviour at high frequency. According to Boucard *et al.*,<sup>28</sup> at low shear rates, the silicate platelets of high aspect ratio are well separated and this strongly increases the viscosity. On the contrary, at higher shear rates the platelets are oriented in the flow direction, which consequently leads to a

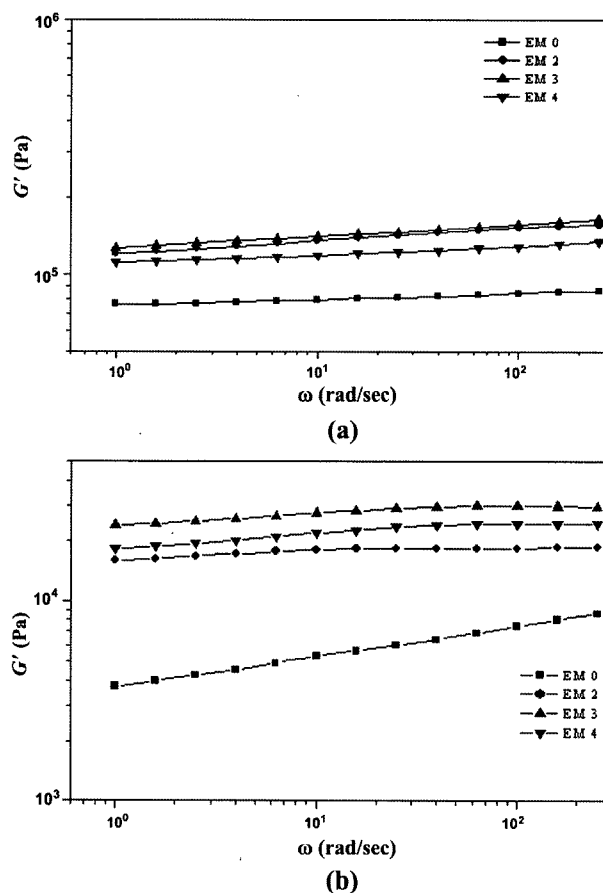


**Figure 4.** Dynamic (a) storage and (b) loss modulus for the EPDM/16Me-MMT nanocomposites.

reduction in the viscosity.

The variation of storage ( $G'$ ) and loss moduli ( $G''$ ) with the frequency for neat EPDM and its nanocomposites are displayed in Figure 4(a) and (b). It clearly shows that the rheological behaviour of neat EPDM is significantly altered when 2 to 4 wt% 16-MMT filler is added to it; indicating that the frequency dependence of ( $G'$ ) and ( $G''$ ) is definitely perturbed by the presence of organomodified clay in EPDM and results in the modification of the classical power laws for the frequency dependence of ( $G'$ ) and ( $G''$ ). It is expected that the temperature and frequencies at which the rheological measurements are carried out, polymeric chains should be fully relaxed and exhibit characteristic homopolymer-like terminal behaviour<sup>29</sup> i.e., for which power law at observed frequencies agrees with expectations for thermoplastic,  $G' \approx \omega$  and  $G'' \approx \omega^2$ . The magnitudes of ( $G'$ ) and ( $G''$ ) are relatively much higher for all EPDM/organoclay nanocomposites compared to the neat EPDM with the effects being more pronounced in ( $G'$ ) than in ( $G''$ ) at all the frequencies under investigation. Such an increase in ( $G'$ ) and ( $G''$ ) are typical of a 'pseudo solid-like' response and is clearly seen in the EPDM nanocomposites. The transition of ( $G''$ ) for all

the nanocomposites shows the nonterminal linear viscoelastic behaviour. Conventionally it may be noted that the solid like response has also been observed in filled polymer systems in which there exist a strong interactions between the polymer and the filler, which is attributed to the presence of yield phenomena in these system.<sup>30</sup> As a result, presence of silicate layers and the lack of complete relaxation of the chains contribute to the pseudo-solid-like response at the frequency ranges under investigation.<sup>31</sup> In the present case,  $G'$  and  $G''$  tends to rise at all the frequency monotonically with increase in nanoclay content up to 3 wt% of organoclay loading and where nanocomposites possess the largest improvement in storage modulus. This is basically due to the disordered nanoclay sheets predominate in the polymer matrix compare to the intercalated silicate sheets with increase in organoclay loading. The disordered organoclay silicate layers interact with the polymer chains and resist its free rotation in the polymer matrix. This incomplete relaxation leads to the formation of percolated network and, thereby, accounts for significant improvements in viscoelastic properties of the EPDM organoclay nanocomposites. However, further addition of 4 wt% of organoclay in EPDM results a decrease in the moduli; which in all probability is due to the increasing tendency of organoclay to undergoing simultaneously intercalation as well as aggregation of silicate layers.<sup>32,33</sup> Thereby, the intermolecular interaction between the silicate layers and polymer chain governs the alteration of the relaxation process of the polymer chain and leads to the low frequency plateau in the shear moduli. The higher the shear moduli and smaller the slope, the more pronounced the interaction between the silicates platelets and their tendency to form a three-dimensional superstructure.<sup>34</sup>

Figure 5 shows the variation of loss tangent ( $\tan\delta$ ) versus frequency ( $\omega$ ) plots for EPDM and its organoclay nanocomposites. It is clear from that the slope of  $\tan\delta$ - $\omega$  plot for the neat EPDM is positive and magnitude of  $\tan\delta$  is relatively much lower compared to its organomodified nanocomposites

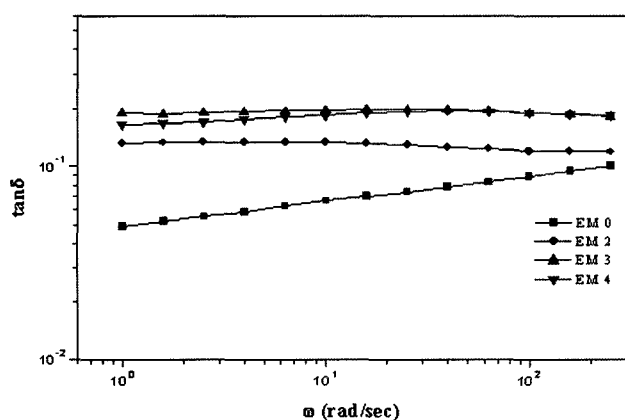


**Figure 5.** The loss tangent ( $\tan\delta$ ) at various wt% of 16Me-MMT content as a function of frequency for nanocomposites.

at all the frequencies. It is also observed that the magnitude of  $\tan\delta$  on adding 2, 3 and 4 wt% of organoclay in EPDM follows the order: EPDM  $\ll$  EM2  $<$  EM4  $<$  EM3. These substantial deviations are related to the terminal flow behaviour and elastic response of the organomodified clay contents in EPDM matrix. The randomly distributed disordered organoclay offers a lesser elastic response than the intercalated organoclay in polymer matrix. However the exfoliated organoclay influence the loss tangent behavior of EPDM nanocomposite containing organoclay loading up to 3 wt%, after which, the intercalated phases predominates in determining the loss tangent behaviour. It also shows that the loss tangent ( $\tan\delta$ ) show very weak frequency dependence with the maxima shifting towards increasingly a higher frequency with increasing clay contents in EPDM nanocomposites.

**Swelling Properties of EPDM/16Me-MMT Nanocomposites.** A cross-linked polymer cannot dissolve because polymer chains are bound together and cannot disentangle. However, it can generally absorb solvent and subsequently swelled in a good solvent.<sup>35</sup> As solvent enters the network, a diluting force develops and the chain must elongate simultaneously on the other hand an elastic retractive force in opposite to this deformation. When these two opposite forces cancelled each other then the steady state is achieved.

Figure 6 shows the variation of toluene uptake versus 16Me-MMT content in EPDM. It is clear that the solvent uptake ability EPDM/16Me-MMT nanocomposites increase with respect to the neat EPDM. These findings are well in agreement with the literature<sup>36</sup> where the introduction of alkylammonium cation in Na-MMT has improved solvent uptake capability for organic solvent molecules, which in turn effectively compete with the organic absorption sites on the organoclay surface. The solvent uptake increases with the addition of organoclay in EPDM and is highest for 3 wt% of organomodified clay and could be account from the relative proportion of disordered and ordered species. The dis-

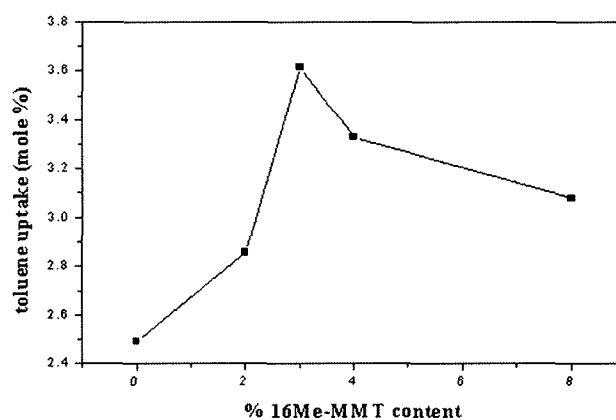


**Figure 6.** Variation of toluene uptake with 16Me-MMT content for EPDM nanocomposites.

ordered nanofillers increase the free volume with addition to decrease in gel fraction and consequently enhance the solvent uptake of EPDM matrix during swelling. At low filler content, the disorder phase dominates<sup>2,37</sup> and the amount of disordered particle is high enough for the 3 wt% clay to promote the highest solvent uptake. At higher filler contents, even up to 8 wt%, the disorderedness tend to decrease and the equilibrium between disorder phase and intercalated phase drawn towards intercalation to result in reduced solvent uptake, though, gel fraction decreases regularly.

The increase in intercalation level thereby promotes lesser free volume in polymer matrix and the formation of polymer-bridging flocculation in solvent,<sup>38</sup> though the possibility of extraction of polymer chains as gel from the silicate inter-layer space cannot be ruled out. It may be noted that due to the steric repulsion between silicate sheets in EPDM/organoclay nanocomposites, the ends of the diffused EPDM chain tend to be adsorbed on both the surfaces of organomodified silicate sheets. The intermolecular interactions of EPDM nanocomposites, similar to high molecular weight PEO and highly branched dendrimer nanocomposites,<sup>39</sup> also expected to result in a bridging between two consecutive silicate platelets. After equilibrium swelling, the bridged EPDM chain stretches out and draws the silicate platelets together with lower interlayer spacing ( $d_{001}$ ) of the samples in presence of toluene molecules as displayed in Figure 7.

The swell ratio of the crosslinked polymer network can be computed by using the equation.

$$q = \frac{w_i + (w_s - w_i)/k}{w_i} \quad (4)$$

where,  $q$  is the swell ratio and  $k$  is the ratio of the densities of the solvent to the polymer.

The cross-links between polymer chains usually resist the solvent molecules to penetrate in the polymer matrix. To observe the effect of aluminosilicate layers on the penetration of liquid molecules, cross-link density (defined as the number of moles of cross-links per unit volume) of nanocomposites

are calculated by the Flory-Rehner equation,<sup>40</sup>

$$-[\ln(1 - V_r) + V_r + \chi V_r^2] = V_0 n \left( V_r^{\frac{1}{3}} - \frac{V_r}{2} \right) \quad (5)$$

where,  $n$  is the cross-link density;  $V_r$  and  $V_0$  are the volume fraction of nanocomposite in the swollen mass and molar volume of solvent ( $V_0$  of toluene = 106.4 cm<sup>3</sup>/mol) respectively;  $\chi$  is the polymer-solvent interaction parameter. The volume fractions ( $V_r$ ) of the nanocomposite in the swollen mass are reverse of the swell ratio<sup>25</sup> i.e.,  $V_r = 1/q$ . The value of  $\chi$  could be obtained from the Flory Huggins's equation.

$$\chi \approx 0.34 + \frac{V_0}{RT} (\delta_s - \delta_p)^2 \quad (6)$$

where,  $\delta_s$  and  $\delta_p$  are solubility parameter of solvent and polymer respectively.<sup>41,42</sup>

Figure 8 represents the influence of aluminosilicate layers on volume fraction ( $V_r$ ) and cross-link density ( $n$ ) of EPDM copolymer during swelling and its nanocomposites with organomodified clay. It shows that the volume fraction,  $V_r$ , and cross-link density,  $n$ , of the nanocomposite in the swol-

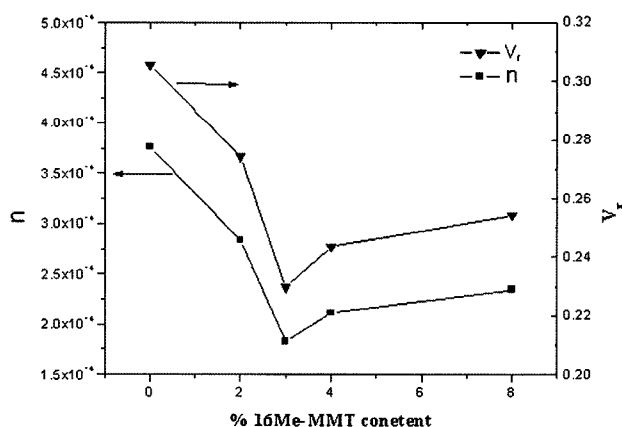


Figure 8. Effect of 16Me-MMT content on volume fraction and cross-link density of EPDM nanocomposites.

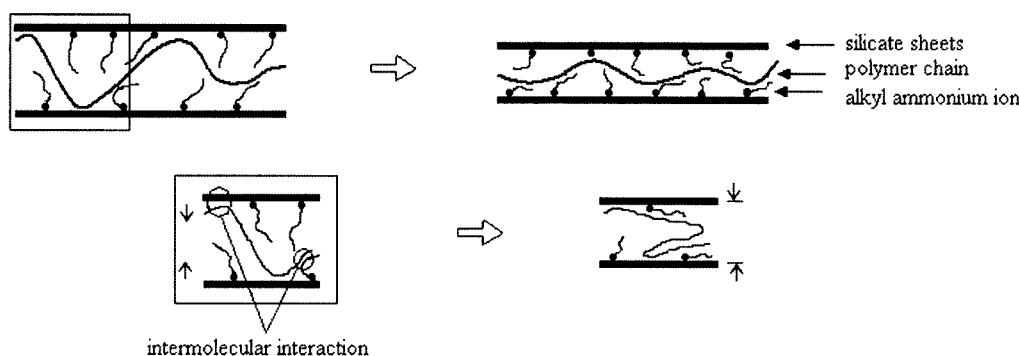


Figure 7. Schematic illustration of bridging flocculation occur in polymer nanocomposites.

len mass decrease up to 3 wt%. Subsequently, it is followed by continuous increase in the volume fraction and cross-link density up to 8 wt% filler contents. But in both the cases,  $V_r$  and  $n$  is lesser in EPDM/organoclay nanocomposites compared to the neat EPDM. It is expected that at the initial stage, presence of higher exfoliated clay level up to 3 wt% reduce the 'bound polymer' and increase the free volume in the EPDM matrix. When solvent molecules penetrate in to the matrix, they can spread apart the flexible polymer chains and imparts high chain mobility. As a result, the solvent can easily penetrate the larger absorption site of the elongated polymer chain and the solvent uptake is more. However, increase in intercalation level above 3 wt% filler inhibits the penetration of solvent molecules through bridging flocculation. In addition, the presence of lesser number of elongated EPDM chains in EPDM/organoclay nanocomposites are expected due to the aggregation of aluminosilicate layers at higher clay content, an observation already confirmed by XRD and TEM.

The swelling of a polymer in a solvent is invariably accompanied by the increase in entropy as well as decrease in Gibb's free energy. In order to find out the effect of nano level dispersion of organomodified clay on EPDM, change in thermodynamic parameters, the entropy of mixing and free energy change of swelling have been calculated using the equations.<sup>43</sup>

$$\Delta S_{sw} = -R(n_s \ln V_s + n_r \ln V_r) \quad (7)$$

$$\Delta G_{sw} = RT(n_s \ln V_s + n_r \ln V_r + \chi n_s V_r) \quad (8)$$

where,  $\Delta S_{sw}$  and  $\Delta G_{sw}$  are the change in entropy and Gibb's free energy during swelling;  $n_s$  and  $n_r$  are the number of moles of solvent and number moles of nanocomposite respectively<sup>35</sup>;  $V_s$  and  $V_r$  are the volume fractions of solvent and EPDM matrix in the swollen mass respectively;  $R$  is universal gas constant ( $R=8.314 \text{ JK}^{-1}\text{mol}^{-1}$ ).

Table II records the values of  $M_c$ ,  $n_r$ ,  $n_s$ ,  $V_r$ ,  $V_s$  and  $n_s/n_r$  which are required in the calculations of the  $\Delta S_{sw}$  and  $\Delta G_{sw}$  of EPDM/clay nanocomposites in toluene at 25 °C and their variations with filler concentration in EPDM is displayed in Figure 9. It clearly shows that, in general, on adding organo-

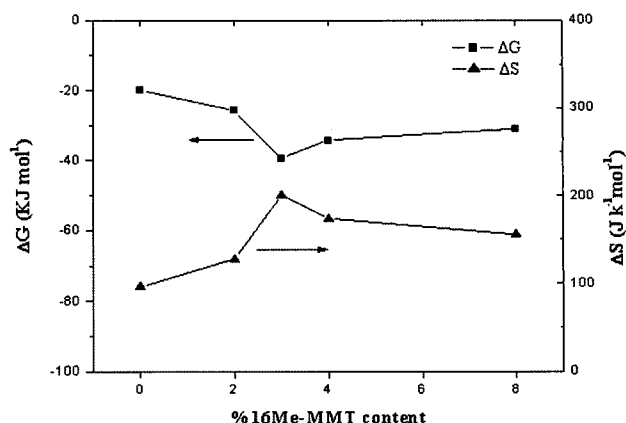


**Figure 9.** Change in entropy of swelling and free energy of swelling as function of 16Me-MMT content for EPDM nanocomposites.

philic clay, free energy change associated with the swelling of polymer decreases while entropy of swelling shows the reverse trend. However, the increase in  $\Delta S_{sw}$  (and decrease in  $\Delta G_{sw}$ ) is highest (lowest) for 3 wt% 16Me-MMT filler in either case. At higher filler contents in EPDM,  $\Delta S_{sw}$  and  $\Delta G_{sw}$  both attains a limiting values. This clearly demonstrates that dispersion of disordered silicate layers up to 3 wt% tends to provide available free volume leading thereby an entanglement of EPDM chains surrounded by silicate layers in swelled polymer. Further addition of filler results in the formation of 'bound polymer' forcing EPDM matrix to undergo relatively lesser swelling in the solvents. A gradual decrease in  $\Delta S_{sw}$  beyond 3 wt% 16-Me-MMT filler concentration in EPDM further strengthens our observation that at higher filler contents, the 'bound polymer' tends to become more and more ordered.

## Conclusions

X-ray diffraction and TEM studies confirmed the disordered-intercalated dispersion nature of organophilic clay in EPDM matrix. Rheological measurement shows a monotonic increase in complex viscosity, storage and loss moduli of nanocomposites with respect to frequency. The properties of

**Table II.** Volume Fraction of EPDM Matrix ( $V_r$ ), Volume Fraction of Toluene ( $V_s$ ), Number of Moles ( $n_r$ ) Related to  $M_c$  of EPDM/Organoclay Nanocomposite in Swollen Mass, Number of Moles ( $n_s$ ) of Toluene, Number Average Molecular Weight between Cross-links ( $M_c$ ) of EPDM/16Me-MMT Nanocomposites

Solvent	Sample*	$V_r$	$V_s$	$M_c$ (gm/mol)	$n_r$ (mol)	$n_s$ (mol)	$n_s/n_r$
Toluene	EM 0	0.3057	0.6943	1,142	$10.692 \times 10^{-5}$	$3.044 \times 10^{-3}$	28.470
	EM 2	0.2743	0.7257	1,533	$6.471 \times 10^{-5}$	$3.988 \times 10^{-3}$	61.63
	EM 3	0.2297	0.7703	2,394	$5.401 \times 10^{-5}$	$4.678 \times 10^{-3}$	86.614
	EM 4	0.2436	0.7564	2,085	$7.099 \times 10^{-5}$	$4.928 \times 10^{-3}$	69.418
	EM 8	0.2543	0.7457	1,920	$7.400 \times 10^{-5}$	$4.373 \times 10^{-3}$	59.095

the nanocomposites have been correlated with the nanodispersion phase of organoclay and their interaction with polymer matrix. The linear viscoelastic properties of EPDM nanocomposites suggest a highest exfoliated dispersion level for 3 wt% of organoclay. With further organoclay loading, the ordered nanodispersion predominates simultaneously with aggregation over the disordered states.

The silicate layers in the nanocomposites containing 3 wt% of organoclay provides a large free volume for toluene insertion. Further increase in organoclay leads to more ordered arrangement and decreases the availability of free volume. The entanglement of the disordered silicate layers in EPDM matrix offers an increase in entropy of swelling. However, for ordered structure, the formation of bound polymer decreases the entropy of swelling.

**Acknowledgements.** The authors are grateful to Ministry of Human Research and Development (MHRD) for the financial support. Authors also gratefully acknowledge Mr. Konstantinos G. Gatos and Prof. József Karger-Kocsis, Institute for Composite Materials Kaiserslautern University of Technology, Kaiserslautern, Germany, for all the help for rheology of the samples.

## References

- (1) Y. Kojima, A. Usuki, M. Kawasumi, A. Okada, Y. Fukushima, and T. Karauchi, *J. Polym. Sci.: Part A: Polym. Chem.*, **31**, 983 (1993).
- (2) M. Alexandre and P. Dubois, *Mater. Sci. Eng.*, **R28**, 1 (2000).
- (3) S. S. Ray and M. Okamoto, *Prog. Polym. Sci.*, **28**, 1539 (2003).
- (4) R. A. Pethrick, in *Polymer-Clay Nanocomposites*, T. J. Pinnavaia and G. W. Beall, Eds., John Wiley & Sons Ltd, Chichester, UK 2002, vol. 51, p. 464.
- (5) K. Gonsalves and X. Chen, in *Materials Research Soc. Symposium Proceedings*, Materials Research Society, Warrendale, PA 1996, vol. 435, p. 55.
- (6) E. P. Giannelis, *Advanced Materials*, **8**, 29 (1996).
- (7) M. Pramanik, S. K. Srivastava, B. K. Samantaray, and A. K. Bhowmick, *J. Polym. Sci.: Part B: Polym. Phys.*, **40**, 2065 (2002).
- (8) K. G. Gatos, N. S. Sawanis, A. A. Apostolov, R. Thomann, and J. Karger-Kocsis, *Macromol. Mater. Eng.*, **289**, 1079 (2004).
- (9) G. Galgali, S. Agarwal, and A. Lele, *Polymer*, **45**, 6059 (2004).
- (10) M. Pramanik, S. K. Srivastava, B. K. Samantaray, and A. K. Bhowmick, *Macromol. Res.*, **11**, 260 (2003).
- (11) S. Su, D. D. Jiang, and C. A. Wilkie, *Polym. Degrad. Stabil.*, **83**, 321 (2004).
- (12) J. Xiao, Y. Hu, Z. Wang, Y. Tang, Z. Chen, and W. Fan, *Eur. Polym. J.*, **41**, 1030 (2005).
- (13) A. Ranade, N. A. D'Souza, and B. Gnade, *Polymer*, **43**, 3759 (2002).
- (14) D. A. Brune and J. Bicerano, *Polymer*, **43**, 369 (2002).
- (15) Y. T. Vu, J. E. Mark, L. H. Pham, and M. Engelhardt, *J. Appl. Polym. Sci.*, **82**, 1391 (2001).
- (16) H. Acharya, M. Pramanik, S. K. Srivastava, and A. K. Bhowmick, *J. Appl. Polym. Sci.*, **93**, 2429 (2004).
- (17) M. Feng, F. Gong, C. Zhao, G. Chen, S. Zhang, and M. Yang, *Polym. Int.*, **53**, 1529 (2004).
- (18) M. Zanetti, G. Camino, D. Canavese, A. B. Morgan, F. J. Lamelas, and C. A. Wilkie, *Chem. Mater.*, **14**, 189 (2002).
- (19) H. J. Walls, J. Zhou, J. A. Yerman, P. S. Fedkiw, S. A. Khan, M. K. Stowe, and G. L. Baker, *J. Power Sources*, **89**, 156 (2000).
- (20) C. W. Macosko, *Rheology: Principles, Measurements, and Applications*, VCH Publisher, New York, 1994.
- (21) J. D. Ferry, *Viscoelastic Properties of Polymers*, 3rd edn., Wiley, New York, 1980.
- (22) Y. H. Hyun, S. T. Lim, H. J. Choi, and M. S. Jhon, *Macromolecules*, **34**, 8084 (2001).
- (23) J. Ren, A. S. Silva, and R. Krishnamoorti, *Macromolecules*, **33**, 3739 (2000).
- (24) E. Manias, G. Hadziioannou, and T. G. Brinke, *Langmuir*, **12**, 4587 (1996).
- (25) G. Schmidt, A. I. Nakatani, P. D. Butler, A. Karim, and C. C. Han, *Macromolecules*, **33**, 7219 (2000).
- (26) L. Onsager, *Ann. NY Acad. Sci.*, **51**, 627 (1949).
- (27) E. A. DiMarzio, A. J. M. Yang, and S. C. Glotzer, *J. Res. Nat. Inst. Stan. Techn.*, **100**, 173 (1995).
- (28) S. Boucard, J. Duchet, J. F. Gérard, P. Prele, and S. Gonzalez, *Macromolecular Symposia*, **194**, 241 (2003).
- (29) R. Krishnamoorti and E. P. Giannelis, *Macromolecules*, **30**, 4097 (1997).
- (30) S. Agarwal and R. Salovey, *Polym. Eng. Sci.*, **28**, 4313 (1995).
- (31) T. A. Witten, L. Leibler, and P. A. Pincus, *Macromolecules*, **23**, 824 (1990).
- (32) T. G. Gopakumar, J. A. Lee, M. Kontopoulou, and J. S. Parent, *Polymer*, **43**, 5483 (2002).
- (33) H. S. Jeon, J. K. Rameshwaram, G. Kim, and D. H. Weinkauff, *Polymer*, **44**, 5749 (2003).
- (34) M. J. Solomon, A. S. Almusallam, K. F. Seefeldt, A. Somwangthanoj, and P. Varadan, *Macromolecules*, **34**, 1864 (2001).
- (35) M. Pramanik, H. Acharya, and S. K. Srivastava, *Macromol. Mater. Eng.*, **289**, 562 (2004).
- (36) K. Ratanarat, M. Nithitanakul, D. C. Martin, and R. Magaraphan, *Rev. Adv. Mater. Sci.*, **5**, 187 (2003).
- (37) R. A. Vaia, in *Polymer-Clay Nanocomposites*, T. J. Pinnavaia and G. W. Beall, Eds., John Wiley & Sons Ltd, Chichester, 2000, p. 229.
- (38) J. Swenson, M. V. Smallry, H. L. M. Hatharasinghe, and G. Fragneto, *Langmuir*, **17**, 3813 (2001).
- (39) M. Murat and G. S. Grest, *Macromolecules*, **29**, 1278 (1996).
- (40) P. J. Flory, *Principles of Polymer Chemistry*, Ithaca, NY, Cornell University, 1953, p. 576.
- (41) *Encyclopedia of Polymer Science and Engineering*, 2<sup>nd</sup> edition, John Wiley & Sons, New York, 1990, vol. 5.
- (42) D. W. Van Krevelen and P. J. Hoftyzer, *Properties of Polymers*, 2<sup>nd</sup> complementary revised edition, Elsevier, New York, 1976.
- (42) D. W. Van Krevelen and P. J. Hoftyzer, *Properties of Polymers*, 2<sup>nd</sup> complementary revised edition, Elsevier, New York, 1976.
- (43) *Encyclopedia of Polymer Science and Engineering*, 2<sup>nd</sup> edition, John Wiley & Sons, New York, 1990, vol. 15.